JOURNAL OF CATALYSIS 133, 498–514 (1992)

Temperature-Programmed Sulfiding of Precursor Cobalt Oxide Genesis of Highly Active Sites on Sulfided Cobalt Catalyst for Hydrogenation and Isomerization

KAZUHIRO INAMURA, TOSHIYUKI TAKYU, YASUAKI OKAMOTO,* KOZO NAGATA,* AND TOSHINOBU IMANAKA*

*Central Research Laboratories, Idemitsu Kosan Co., Ltd., 1280 Kamiizumi, Sodegaura, Chiba 299-02; and *Department of Chemical Engineering, Faculty of Engineering Science, Osaka University, Toyonaka, Osaka 560, Japan*

Received May 6, 1991; revised August 12, 1991

It was found that the method of sulfidation of cobalt oxide strongly affects the catalytic activities and selectivities of the resultant cobalt sulfide catalyst, as well as the calcination temperature of the cobalt oxide. When cobalt oxide was sulfided at 673 K by a temperature-programmed sulfiding method (a heating rate of 6 K min^{-1}), catalytic activities for the hydrogenation of butadiene and the isomerization of 1-butene were considerably enhanced compared with those for cobalt sulfide prepared by isothermal sulfidation at 673 K. Results of temperature-programmed sulfiding (TPS), temperature-programmed reduction (TPR), and X-ray diffraction (XRD) suggest that the catalysts showing high catalytic activities after sulfidation are partially sulfided at 673 K and consist of the unsulfided cobalt core phases (CoO or metallic Co). The sulfidation property of precursor cobalt oxides has been studied using TPS, simulating the sulfidation process of the cobalt sulfide catalysts. Two distinctly different kinds of sulfidation process are estimated by TPS measurements of the cobalt oxides. The calcination temperature of the precursor cobalt oxides strongly affects the sulfidation paths. They are differentiated in terms of the presence of a metallic Co intermediate. The relationship of the mechanism of sulfidation of the cobalt oxides to the generation of highly active sites is discussed.

INTRODUCTION

Recently, the catalytic activity and structure of cobalt sulfide have received much attention in connection with synergies between Co and Mo in hydrodesulfurization (HDS) reactions. For example, de Beer and co-workers (*1*) and Ledoux *et al.* (*2*) reported that the high HDS activity of Co–Mo catalysts was attributed to the high activity of Co sites optimally dispersed and modified on molybdenum sulfides. Furthermore, de Beer and co-workers (*1, 3*) demonstrated that carbon-supported cobalt sulfide catalysts showed much higher HDS activity than carbon- or Al_2O_3-supported molybdenum catalysts. They proposed that the role of MoS_2 in Co–Mo catalysts was mainly to function as a support for the catalytically active Co species.

We have reported previously that the calcination temperature of precursor cobalt oxide significantly affects the catalytic activities and selectivities of resultant sulfide catalysts for the hydrogenation of butadiene and the isomerization of 1-butene (*4*). It has also been revealed that the particle size of the precursor cobalt oxide and the sulfidation conditions determine the catalytic properties of the sulfide catalysts (*4*). In particular, extremely enhanced catalytic activities were found for the cobalt sulfide catalysts prepared from cobalt oxide calcined at temperatures over 1473 K. A model for these high active sites, denoted "Co(H)", was proposed as cobalt metal overlayers modified by sulfur. Co(H) sites showed essentially identical characteristics of butadiene

[1] To whom correspondence should be addressed.

0021-9517/92 $3.00

hydrogenation with a "type B" behavior of sulfided cobalt metal described by Wells and co-workers (*5*). However, the mechanism of generation of the catalytic active sites remains obscure because of the difficulty in understanding the sulfidation processes.

Only in the past decade, Arnoldy, Moulijn, and co-workers established a significant development for understanding the sulfidation properties of Co- and Mo-containing catalysts, mainly by temperature-programmed sulfiding (TPS) technique (*6–8*). TPS provides more useful information on the sulfidation process than other spectroscopic techniques. TPS can easily simulate actual sulfidation procedures (or activation processes) and TPS patterns can provide both qualitative and quantitative information on the sulfidation reaction simultaneously.

We systematically examine the sulfidation properties of the precursor cobalt oxides calcined at various temperatures (T_c = 573–1573 K) by using mainly TPS. In the present study, the activities and selectivities for hydrogenation and isomerization are also examined for the cobalt catalysts sulfided by two different kinds of sulfidation methods. The sulfidation method is found to strongly affect the amount of Co(H) sites and thus the T_c dependence of the catalytic activities and selectivities.

EXPERIMENTAL

Catalyst Preparation

A detailed description of the preparation of cobalt oxides has been given elsewhere (*4*). The cobalt oxide, which was prepared by decomposing cobalt acetate in air at 573 K for 5 h, was again calcined at varying temperatures (T_c = 573–1573 K) for 5 h. The cobalt oxide was ground into fine powder using a mortar and pestle. The cobalt oxide calcined at T_c is denoted Co–O(T_c). X-Ray diffraction patterns showed exclusive formation of Co_3O_4 irrespective of T_c.

Sulfidation of the cobalt oxides was conducted by two methods. One, denoted isothermal sulfidation, is described elsewhere (*4*). The oxide sample in a reaction cell was exposed in a stream of atmospheric pressure of H_2S/H_2 (molar ratio: $\frac{1}{10}$, 550 cm^3 min^{-1}) at 673 K for 90 min after brief evacuation at room temperature. Subsequently, the sulfided sample was treated for 60 min at 673 K in a stream of atmospheric pressure of H_2 (500 cm^3 min^{-1}).

The other sulfidation method is denoted temperature-programmed sulfidation. The oxide sample in the cell was first exposed to H_2S/H_2 ($\frac{1}{10}$, atmospheric pressure, 550 cm^3 min^{-1}) at room temperature and the temperature was increased continuously at a heating rate, β, of 6 K min^{-1} up to 673 K. Subsequently, the sample was further sulfided for 90 min at 673 K, followed by an H_2 treatment for 60 min at 673 K in the same way as for the isothermal sulfidation.

The cobalt sulfide catalyst prepared from Co–O(T_c) by isothermal sulfidation is designated Co–S_{iso}(T_c), where S_{iso} refers to the isothermal sulfidation. Similarly, the cobalt catalyst sulfided from Co–O(T_c) by temperature-programmed sulfidation is designated Co–S_{pro}(T_c), where S_{pro} refers to temperature-programmed sulfidation.

Catalytic Activity

Both hydrogenation of butadiene (H_2/butadiene molar ratio: $\frac{2}{1}$) and isomerization of 1-butene (H_2/butene: $\frac{1}{1}$) were carried out over the cobalt sulfide catalyst (ca. 0.3 g) at 473 K and a total pressure of 0.15 bar using a closed circulation system (220 cm^3). The reaction gases were analyzed by GLC using a column packing of sebaconitrile. Further details of the activity measurements are given in the previous paper (*4*).

Temperature-Programmed Sulfiding

The principle of the TPS methods has been described by Moulijn and co-workers (*6–9*). The TPS/TPR apparatus used here has the same construction as reported by them. A scheme of the apparatus is shown in Fig. 1. The sulfiding gases were prepared by mixing streams of 64.5% H_2/Ar [flow rate

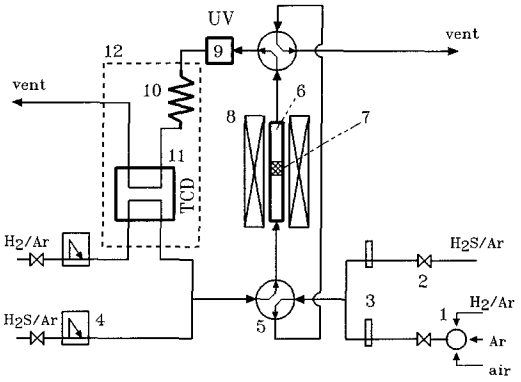

FIG. 1. Schematic representation of equipment used in temperature-programmed studies. Designations: (1) gas select valve, (2) stop valve, (3) flow controller, (4) mass-flow controller, (5) four-way valve, (6) reactor, (7) catalyst bed, (8) electric furnace, (9) UV spectrophotometer, (10) molecualr sieve (MS-5A) trap, (11) thermal conductivity detector (TCD), (12) thermostat.

5.00 cm^3 min^{-1}, purified by passage over both a moisture purifier and an oxygen purifier (Gasukuro Kogyo Inc., Gas Clean Filter)] and 5.44% H_2S/Ar (9.42 cm^3 min^{-1}, not further purified). The composition of the resulting gases was ca. 3.6% H_2S, 22.4% H_2, and 74.0% Ar. The total pressure of the gases in the reactor was regulated at 1.18 bar.

The H_2S concentration in the reactant gases was analyzed with a UV spectrophotometer (Japan Spectroscopic Co., Ltd., 875-UV). Although H_2S in the sulfiding gases has a strong absorption band around 196 nm, the H_2S concentration (ca. 3.6%) is too high to monitor its absorption signal at 196 nm with the UV detector. Thus, the UV spectrophotometer was set at 212 nm to give a linear relationship between the H_2S concentration and its absorption signal under our TPS conditions. The H_2 concentration was determined with a thermal conductivity detector (TCD; Ohkura Riken Co., Ltd., Model 802T), after H_2S and H_2O had been trapped in a 5A molecular sieve trap. The TCD and the molecular sieve trap were thermostated at 313 ± 0.1 K.

The experimental procedures for TPS measurements are as follows. The oxide sample in a quartz tube reactor (internal diameter of 6 mm) was purged with a pure Ar flow at 300 K for more than 60 min. Then the Ar flow was replaced with the sulfiding gases at 300 K for 90 min. Subsequently, the temperature was increased up to a desired temperature (T_s, max 1350 K) at a constant heating rate (β = 10, 6, or 2 K min^{-1}), followed by isothermal sulfidation at T_s. The reactor charge was typically 8 mg of Co_3O_4 for β = 10 K min^{-1}, 16 mg for β = 6 K min^{-1}, and 29 mg for β = 2 K min^{-1}. The UV spectrometer and the TCD were calibrated by sulfidation of a known amount of Fe_2O_3 (Rare Metallic Co., Ltd., 99.999%), assuming complete sulfidation to FeS under the TPS condition (H_2/H_2S = 0.16, T_s = 1350 K) (*12*). Only the crystalline phase of FeS (troilite) was observed by X-ray diffraction of the sulfided Fe_2O_3 at 1350 K. The sensitivity of the UV response for a mole of H_2S was ca. 1.7 times higher than that of the TCD response for a mole of H_2 in the TPS experiments. All TPS charts are shown in this sensitivity ratio unless otherwise noted.

In some cases, sequential experiments of TPS and TPR for the cobalt catalysts were conducted using the same reactor cell. After the TPS procedure, the reactor was cooled to 300 K in the sulfiding gases, and then replaced with Ar (20 cm^3 min^{-1}) at 300 K for more than 60 min. Sequentially, the temperature increased from 300 to 1350 K at β = 10 K min^{-1} in a stream of 64.5% H_2/Ar (20 cm^3 min^{-1}) after the Ar was replaced with H_2/Ar at 300 K for 90 min (TPR mode). H_2 consumption and H_2S evolution on reduction were also measured with the TCD and the UV spectrophotometer, respectively. As the detectable H_2S was considerably of lower concentration in the TPR mode, the UV spectrophotometer was set at 202 nm instead of 212 nm for the TPS mode. Thus, H_2S detection in the TPR mode had higher sensitivity than that in the TPS mode. It is noteworthy that the H_2S response at 202 nm is little affected by H_2O, which has an absorption maximum around 167 nm (*10*). The absolute sensitivity of the

TCD was determined by the reduction of high-purity V_2O_5, assuming complete reduction to V_2O_3 at 900 K (*11*). Subsequently, the UV spectrophotometer was calibrated by reduction of a known amount of MoS_2 (Rare Metallic Co., Ltd., >99%), which was used after sulfidation at 650 K for 2 h to eliminate the oxidic moiety formed in atmospheric oxygen. Under our TPR condition, total H_2 consumption of MoS_2 was in fair agreement with that required for complete reduction to Mo metal at 1350 K, while the degree of reduction of MoS_2 has been reported to be 90% at 1250 K (*9*). The sensitivity of the UV response for a mole of H_2S was ca. 2.1 times higher than that of the TCD response for a mole of H_2 in the TPR experiments.

XRD patterns of the calcined and sulfided catalysts were obtained using a Shimazu VD-1 diffractometer employing Cu$K\alpha$ radiation with a Ni filter. XRD measurements of the sulfided catalysts were conducted in air as soon as possible after the treatments. The crystallite sizes of Co_3O_4 and Co_9S_8 were estimated from the linewidths using Scherrer's equation ($K = 0.9$). A correction was made for instrumental line broadening.

RESULTS

Catalytic Activity

BET surface areas and crystallite sizes of the cobalt oxide [Co–O(T_c)] and cobalt sulfide obtained by isothermal sulfidation [Co–S_{iso}(T_c)] were given in the previous paper (*4*) and are summarized in Table 1. The catalytic activities of Co–S_{iso}(T_c) as a function of calcination temperature T_c for the precursor oxide have also been described in the previous paper (*4*). It has been demonstrated that the calcination temperature of the precursor oxide strongly affects the activity of the resultant sulfide catalysts. In this study, we plan to elaborate on the catalytic activities of the cobalt sulfide obtained by temperature-programmed sulfidation [Co–S_{pro}(T_c)].

As shown in Table 1, the surface areas of the cobalt oxides decreased greatly as T_c increased from 573 to 1173 K and more gradually at higher T_c. The T_c dependence of the surface area is consistent with that of the crystallite size of Co_3O_4. The crystallite sizes of Co–S_{iso}(T_c), on the other hand, decrease with increasing T_c, contrary to the change in surface areas, suggesting the formation of a noncrystalline cobalt sulfide phase (*4*). The surface areas of Co–S_{pro}(T_c) are 2.5–4 times lower than those of Co–S_{iso}(T_c).

Activities and selectivities of Co–S_{pro}(T_c) are presented in Tables 2 and 3. Figures 2 and 3 illustrate the catalytic activities of Co–S_{pro}(T_c) as a function of T_c for the hydrogenation of butadiene and the isomerization of 1-butene, respectively. The activities of Co–S_{iso}(T_c) are also shown for comparison. Activities of Co–S_{iso}(T_c) are invariant with increasing T_c up to 1273 K and then sharply increase, whereas the Co–S_{pro}(573–1573 K) have maximum activity for the hydrogenation at T_c = 1373 K. The hydrogenation activity of Co–S_{pro}(T_c) is 10- to 13-fold higher than that of Co–S_{iso}(T_c) at T_c = 1173–1373 K. The variation in activities of Co–S_{iso}(T_c) and Co–S_{pro}(T_c) for the isomerization is similar to that for the hydrogena-

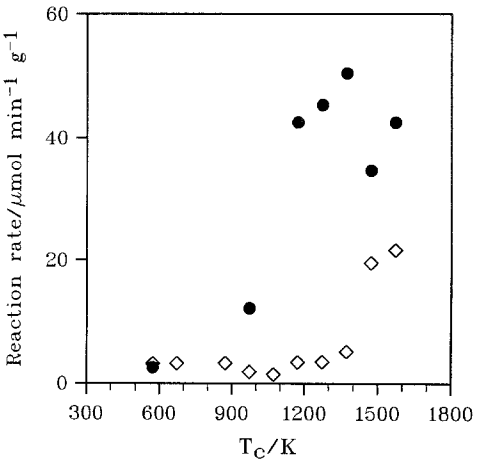

FIG. 2. Reaction rates of the hydrogenation of butadiene at 473 K as a function of the calcination temperature T_c of the precursor cobalt oxide for cobalt sulfide catalysts: ◇, Co–S_{iso}(T_c); ●, Co–S_{pro}(T_c).

TABLE 1

BET Surface Areas and Crystallite Sizes of Cobalt Oxide and Sulfide

T_c (K)	BET surface area ($m^2\ g^{-1}$)			Crystallite size[a] (nm)	
	Co–O	Co–S_{iso}[b]	Co–S_{pro}[c]	Co–O	Co–S_{iso}[b]
573	14.1	38	9	14	48
973	3.2	24	7	64	
1073	0.71				
1173	0.41	41		79	31
1473	0.21	17	4	113	20
1573	0.17	11	4.5	113	19

[a] Crystallite diameters of Co_3O_4 ($2\theta = 36.9°$) and Co_9S_8 ($2\theta = 52.9°$) for oxide and sulfide, respectively.

[b] Sulfided at 673 K by isothermal sulfidation and H_2 treatment at 673 K.

[c] Sulfided at 673 K by temperature-programmed sulfidation and H_2 treatment at 673 K.

tion. These results indicate that the temperature-programmed sulfidation (or gradual sulfidation) for the precursor cobalt oxide brings about higher catalytic activities for both hydrogenation and isomerization than those for the isothermal sulfidation (or rapid sulfidation).

As seen in Tables 2 and 3, the cobalt sulfide exhibiting high hydrogenation activity shows a high *trans*-2-butene selectivity in contrast to a high 1-butene selectivity over Co–S_{pro}(573 K) with a low activity. The relationship between hydrogenation activity and selectivity for Co–S_{pro}(T_c) is consistent with that for Co–S_{iso}(T_c) (*4*). This is also the case for the relationship between isomerization activity and selectivity.

Temperature-Programmed Sulfiding (β = 10 K min^{-1})

Figure 4 shows two typical TPS patterns of cobalt oxides calcined at 573 and 1573 K

TABLE 2

Reaction Rates and Initial Selectivities of the Hydrogenation of Butadiene over Cobalt Sulfide Catalysts[a] Prepared from Cobalt Oxides Calcined at Various Temperatures

Catalyst (T_c)	Reaction rate[b]	Initial selectivity[c] (%)		
		1-Butene	*trans*-2-Butene	*cis*-2-Butene
Co–S_{pro}(573 K)	2.55	69.3	22.9	7.8
Co–S_{pro}(973 K)	12.2	49.2	44.7	6.1
Co–S_{pro}(1173 K)	42.5	24.9	68.7	6.4
Co–S_{pro}(1273 K)	45.3	25.3	67.5	7.2
Co–S_{pro}(1373 K)	50.4	25.2	66.5	8.3
Co–S_{pro}(1473 K)	34.6	24.1	68.5	7.4
Co–S_{pro}(1573 K)	42.5	22.9	65.6	11.5

[a] Co–S_{pro}(T_c) was prepared from the cobalt oxide calcined at T_c and sulfided at 673 K by temperature-programmed sulfidation and H_2 treatment at 673 K.

[b] At 473 K, 10^{-6} mol min^{-1} g cat^{-1}.

[c] At 473 K. Only a negligible amount of butane was observed.

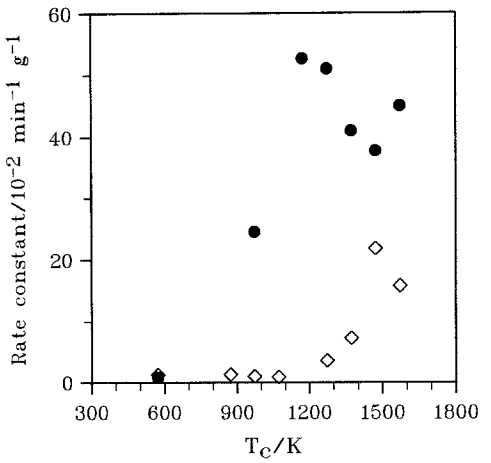

FIG. 3. Rate constants of the isomerization of 1-butene at 473 K as a function of the calcination temperature T_c of the precursor cobalt oxide for cobalt sulfide catalysts: ◇, Co–$S_{iso}(T_c)$; ●, Co–$S_{pro}(T_c)$.

(β = 10 K min^{-1}). These TPS patterns are divided into two regions: (I) sulfidation of Co_3O_4 to Co_9S_8 at 400–900 K, and (II) interconversions of cobalt sulfide species at 900–1350 K. Similar TPS patterns were reported by Arnoldy *et al.* for the crystalline compounds CoO and Co_3O_4 (*8*). In region I, H_2S consumption is observed at temperatures as low as 400 K and is accompanied by a simultaneous H_2 consumption for Co–O(573 K). With Co–O(1573 K), on the other hand, a precipitous H_2S consumption is observed at ca. 600 K, accompanying a strong H_2 consumption followed by an H_2 evolution. Despite remarkable differences in the TPS patterns in region I, the overall H_2S and H_2 uptakes due to sulfiding are estimated to be identical. Considering the thermodynamic stability of Co_9S_8 (*13–15*), both Co–O(573 K) and Co–O(1573 K) are considered to be sulfided to Co_9S_8 until 900 K but in different sulfidation pathways. It is confirmed that the TPS patterns in region II are in excellent agreement with each other. The interconversions of the cobalt sulfide have been explained to proceed from Co_9S_8 to CoS_{1+x} at temperatures > 1000 K, and subsequently to $Co_4S_{3\pm x}$ or liquid phase at temperatures > 1150 K during the sulfidation (*8, 15*).

The sulfidation property of supported cobalt oxide was compared with that of unsupported cobalt oxide by using TPS. The TPS

TABLE 3

Rate Constants and Initial Selectivities of the Isomerization of 1-Butene over Cobalt Sulfide Catalysts[a] Prepared from Cobalt Oxides Calcined at Various Temperatures

Catalyst (T_c)	Rate constant, k[b]	Initial selectivity[c] (*cis*-2-butene/*trans*-2-butene)
Co–S_{pro}(573 K)	0.83	0.83
Co–S_{pro}(973 K)	24.6	0.73
Co–S_{pro}(1173 K)	52.7	0.73
Co–S_{pro}(1273 K)	51.0	0.72
Co–S_{pro}(1373 K)	41.0	0.75
Co–S_{pro}(1473 K)	37.7	0.73
Co–S_{pro}(1573 K)	45.0	0.73

[a] Co–$S_{pro}(T_c)$ was prepared from the cobalt oxide calcined at T_c and sulfided at 673 K by temperature-programmed sulfidation and H_2 treatment at 673 K.

[b] At 473 K, k = 10^{-2} min^{-1} g cat^{-1}.

[c] At 473 K.

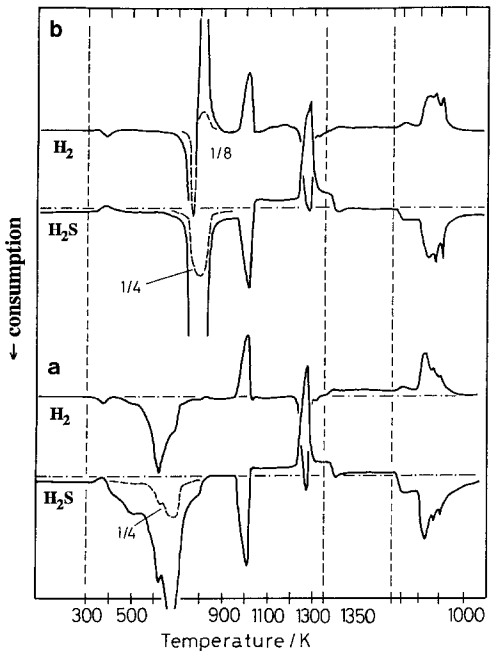

FIG. 4. Temperature-programmed sulfiding patterns of cobalt oxide at β = 10 K min^{-1} (a) Co–O(573 K), (b) Co–O(1573 K). The upper part and lower part of each pattern represent the TCD and UV (212 nm) signals. Negative peaks indicate H_2 and H_2S consumption, respectively.

patterns for CoO/SiO_2 catalyst (10 wt% CoO) prepared from cobalt nitrate (*16*) are shown in Fig. 5. In analogy with the TPS of Co–O(573 K), both H_2S and H_2 consumption peaks are observed concurrently, but these consumption peaks are almost completed up to 600 K.

Temperature-Programmed Sulfiding (β = 2 K min^{-1})

TPS experiments with cobalt oxides were conducted at a lower heating rate (2 K min^{-1}) to elucidate the differences between TPS profiles of Co–O(573 K) and Co–O(1573 K) (Fig. 4). Figure 6 shows the TPS patterns for Co–O(573–1573 K) at β = 2 K min^{-1}. A set of H_2S consumption and H_2 evolution peaks attributable to the interconversion of Co_9S_8 to CoS appear at 990 K in all cases. At sulfidation temperatures between 300 and 900 K, at least five distinctly different sets of H_2S and H_2 peaks are observed at 350–500 K (S0, H0), 550–575 K (S1, H1), 624–665 K (S2, H2), 690–705 K (S3, H3), and 715–777 K (S4, H4). They are denoted S*x* and H*x* for H_2S and H_2 peaks, respectively, where *x* (0–4) refers to the number of peaks with increasing sulfidation

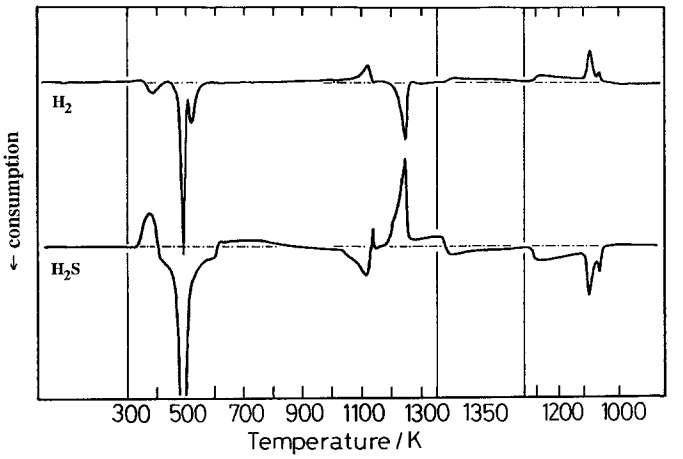

FIG. 5. Temperature-programmed sulfiding patterns of CoO/SiO_2 catalyst (10 wt% CoO) prepared from cobalt nitrate at β = 10 K min^{-1}. The upper part and lower part of each pattern represent the TCD and UV (212 nm) signals. Negative peaks indicate H_2 and H_2S consumption, respectively.

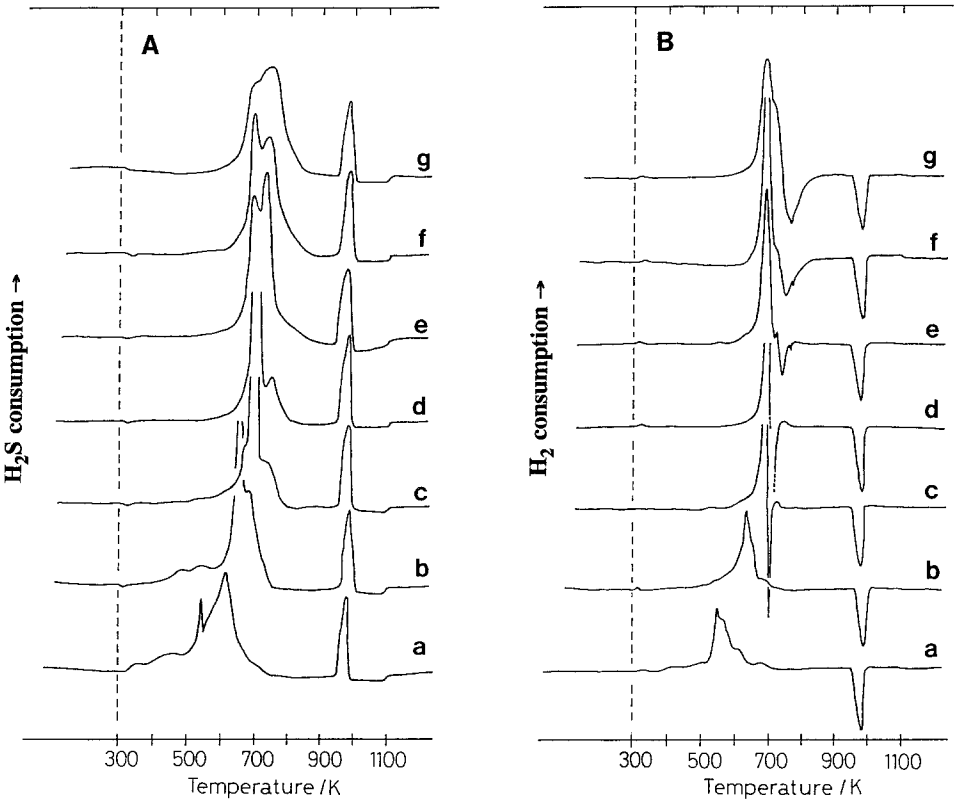

FIG. 6. (A) Temperature-programmed sulfiding patterns (H_2S) of cobalt oxide at $\beta = 2$ K min^{-1}. (a) Co–O(573 K), (b) Co–O(973 K), (c) Co–O(1073 K), (d) Co–O(1173 K), (e) Co–O(1273 K), (f) Co–O(1473 K), (g) Co–O(1573 K). (B) Temperature-programmed sulfiding patterns (H_2) of cobalt oxide at $\beta = 2$ K min^{-1}. (a) Co–O(573 K), (b) Co–O(973 K), (c) Co–O(1073 K), (d) Co–O(1173 K), (e) Co–O(1273 K), (f) Co–(1473 K), (g) Co–O(1573 K).

temperature. Figures 7 and 8 show the variation in the positions of the H_2S consumption and the H_2 consumption/evolution peaks, respectively, as a function of calcination temperature of the precursor cobalt oxide. The variation in the intensity (peak area) of H_2S consumption peaks (S0–4) is also illustrated in Fig. 9.

The lowest sulfidation peak, S0, is observed at ca. 350–500 K for Co–O(573 K) accompanied by a weak H_2 consumption peak, H0. These peaks can hardly be detected for Co–O($T_c \geq 973$ K). In the case of Co–O(573 K) and Co–O(773 K) (not shown in Fig. 6) the peak intensity for H_2 consumption in H1 appeared around ca. 550 K and is obviously larger than that for H_2S consumption in S1. Thus, H_2 consumption is estimated to exceed H_2S consumption in quantity in this temperature range. The H_2S consumption peak, S2, is dominant for Co–O(573), Co–O(773), and Co–O(973). The intensities of S2 for the above three samples are nearly constant (ca. 60% of total H_2S consumption). On the other hand, the corresponding H_2 consumption peak, H2, increases in intensity as T_c increases [ca. 28% of total H_2 consumption for Co–O(573 K) and 77% for Co–O(973 K)]. At $T_c \geq 1073$ K the H_2S consumption is composed of mainly two peaks, S3 and S4. S4 increases at the expense of S3 as T_c increases. On the other hand, the H_2 consumption peak, H3, appears at ca. 700 K. The intensity of H3

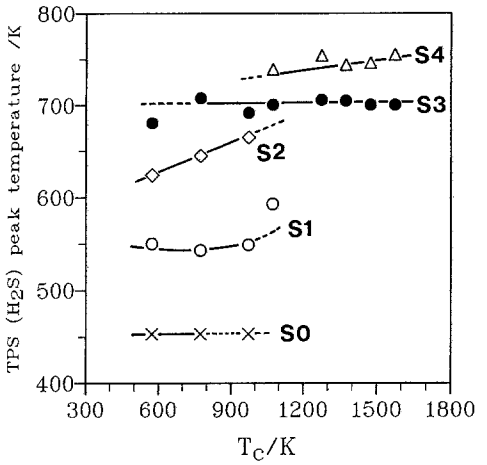

FIG. 7. Positions of the H_2S consumption peak maxima (UV signals, TPS in Fig. 6A) as a function of calcination temperature T_c of the precursor cobalt oxide.

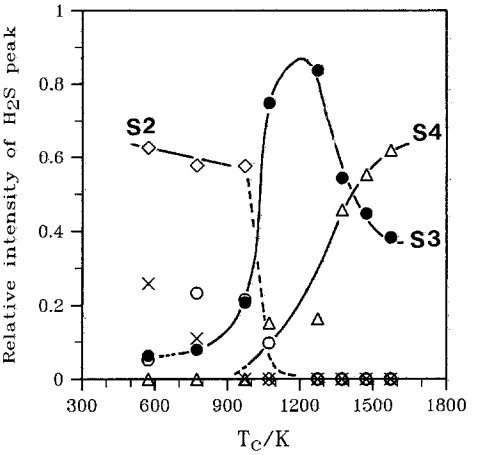

FIG. 9. Dependence of the intensity of the H_2S consumption peak (TPS in Fig. 6A) on the calcination temperature T_c of the precursor cobalt oxide. X, S0; ○, S1; ◇, S2; ●, S3; △, S4.

precipitously increases at $T_c \geq 1073$ K. The H_2 evolution peak, H4, appears and shifts from 715 to 777 K as T_c increases from 1073 to 1573 K.

Sulfidation of Co–O(T_c) to Co–S_{pro}(T_c)

Figure 10 depicts the TPS patterns of Co–O(T_c) at sulfidation temperatures up to 673 K (β = 6 K min^{-1}), followed by isothermal sulfidation at 673 K for 90 min. This TPS procedure corresponds to the sulfidation of Co–O(T_c) to Co–S_{pro}(T_c), except for the subsequent H_2 treatment. It is found that the sulfidation of Co–O(573 K) is nearly completed up to 673 K, whereas the other cobalt oxides are mainly sulfided during the isothermal stage at 673 K. In the case of Co–O(573 K) and Co–O(973 K), peak positions for both H_2S and H_2 consumption are shifted to higher temperatures, compared with the TPS patterns (β = 2 K min^{-1}) in Fig. 6. Such temperature shifts are dependent on the heating rate in TPS measurements. The higher heating rate causes the temperature shifts of peak positions (*17*).

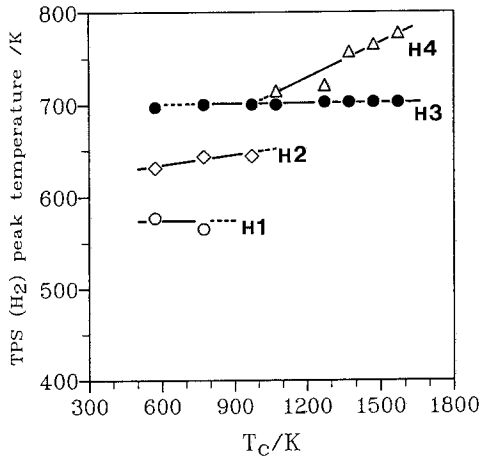

FIG. 8. Positions of the H_2 consumption peak maxima (TCD signals, TPS in Fig. 6B) as a function of calcination temperature T_c of the precursor cobalt oxide.

The H_2 evolution peaks appear apparently for Co–O(1273 K) and weakly for Co–O(1073 K). It is found in separate experiments that the sample size of the cobalt oxide significantly influences the H_2 evolution peak in both intensity and shape. However, total H_2S and H_2 consumptions (determined by peak area measurements over the whole TPS patterns) per mole of Co are almost invariant with sample size. Quantitative TPS results and H_2S and H_2 consumption are summarized in Table 4. An ideal

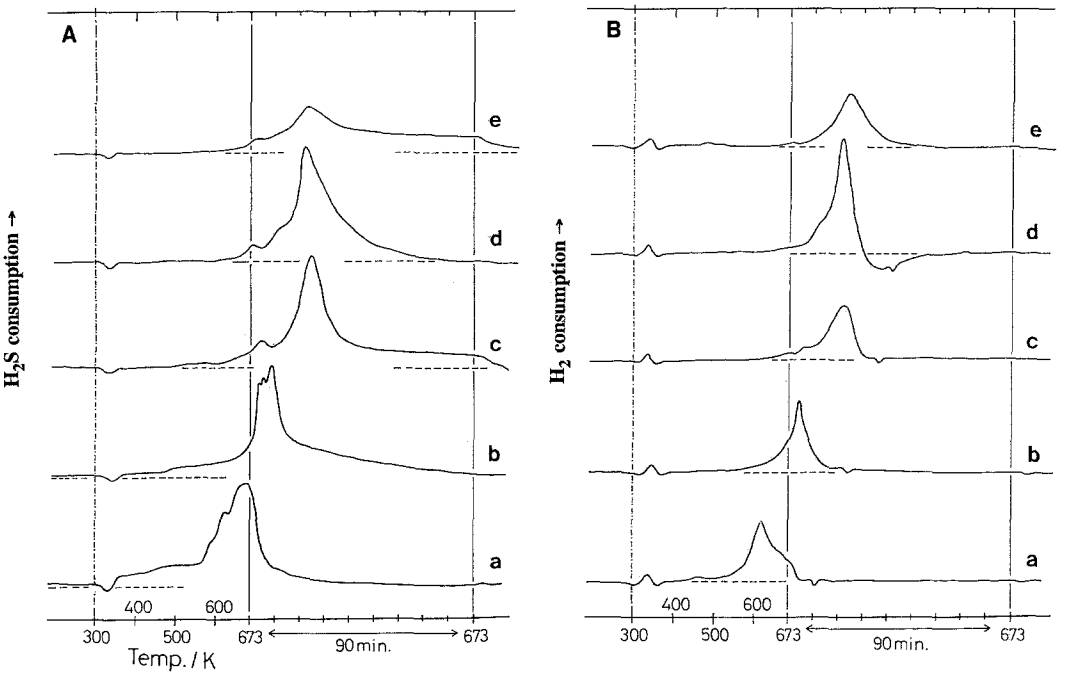

FIG. 10. (A) Temperature-programmed sulfiding patterns (H_2S) of cobalt oxide up to 673 K at β = 6 K min^{-1}, followed by isothermal sulfiding at 673 K for 90 min. (a) Co–O(573 K), (b) Co–O(973 K), (c) Co–O(1073 K), (d) Co–O(1273 K), (e) Co–O(1473 K). (B) Temperature-programmed sulfiding patterns (H_2) of cobalt oxide up to 673 K at β = 6 K min^{-1}, followed by isothermal sulfiding at 673 K for 90 min. (a) Co–O(573 K), (b) Co–O(973 K), (c) Co–O(1073 K), (d) Co–O(1273 K), (e) Co–O(1473 K).

sulfidation of Co_3O_4 to Co_9S_8 is shown as follows, neglecting reaction intermediates.

$$3Co_3O_4 + 8H_2S + 4H_2 \rightarrow Co_9S_8 + 12H_2O. \quad (1)$$

In this case, total H_2S and H_2 consumption, H_2S/Co (mol/mol) and H_2/Co, should be estimated to be 0.89 and 0.44, respectively.

TABLE 4

Total H_2S and H_2 Consumption in TPS[a] of Cobalt Oxide

Cobalt oxide (T_c)	H_2S/Co (mol/mol)	H_2/Co (mol/mol)	H_2S/H_2 (mol/mol)
Co–O(573 K)	0.89	0.46	1.9
Co–O(973 K)	0.93	0.49	1.9
Co–O(1073 K)	0.84	0.45	1.9
Co–O(1273 K)	0.81	0.49	1.7
Co–O(1473 K)	0.77	0.64	1.2

[a] Sulfiding started at 300 K up to 673 K at β = 6 K min^{-1}, followed by an isothermal stage at 673 K for 90 min as shown in Fig. 10.

The results of H_2S/Co, H_2/Co, and H_2S/H_2 shown in Table 4 indicate that the cobalt oxides are completely sulfided to Co_9S_8 in the TPS experiments for Co–O(573–973 K). On the other hand, the H_2S/H_2 consumption ratio is considerably decreased to 1.7 and 1.2 for Co–O(1273 K) and Co–O(1473 K), respectively.

Figure 11 illustrates the typical TPR patterns of the sulfided cobalt samples in TPS experiments in Fig. 10. There are three sets of H_2S evolution/H_2 consumption peaks, denoted α, β, and γ with increasing reduction temperature. The α peak (only an H_2S evolution peak) at ca. 445 K decreases in intensity as T_c increases. Since no H_2 consumption peak appears in this temperature range, the α peak is assigned to desorption of H_2S or recombination of surface SH groups, which adsorb on surface defect sites of the cobalt sulfide particles. The β peak

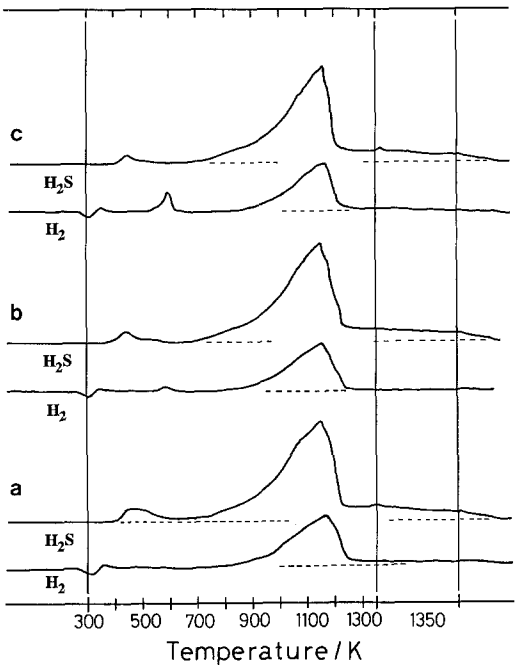

FIG. 11. Temperature-programmed reduction patterns of the sulfided cobalt oxide after the TPS procedure in Fig. 10: (a) Co–O(973 K), (b) Co–O(1273 K), (c) Co–O(1473 K). The upper part and lower part of each pattern represent the UV (202 nm) and TCD signals. Positive peaks indicate H_2S evolution and H_2 consumption, respectively.

(only an H_2 consumption peak) is observed at ca. 600 K for the sulfided Co–O(1273 K) and Co–O(1473 K) in TPS. This is attributable to reduction of the remaining cobalt oxide, probably CoO. Bulk CoO gives one sharp reduction peak at 610 K in TPR (*11*).

TABLE 5

H_2S Evolution and H_2 Consumption in TPR of Cobalt Sulfide[a]

Parent cobalt oxide (T_c)	H_2S evolution[b]		H_2 consumption[c]		
	α	γ	α	β	γ
Co–O(973 K)	3.6	62.7	0.7	0	67.9
Co–O(1273 K)	1.9	57.5	0	1.3	52.7
Co–O(1473 K)	1.3	51.6	0	4.3	49.8

[a] Sulfided of Co–O(T_c) in TPS at 673 K for 90 min (β = 6 K min^{-1}).
[b] H_2S evolution is expressed as 10^{-2} mol H_2S/mol Co.
[c] H_2 consumption is expressed as 10^{-2} mol H_2/mol Co.

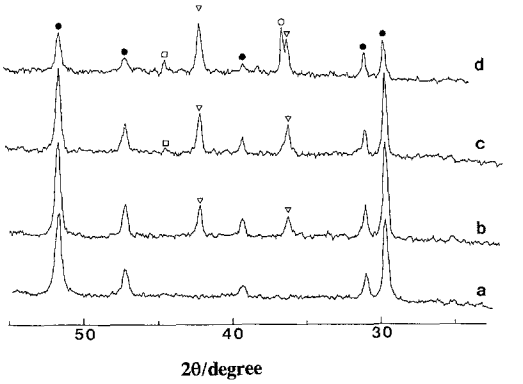

FIG. 12. X-ray diffraction patterns of sulfided Co–O(T_c) in a temperature-programmed sulfidation mode up to 673 K at β = 6 K min^{-1}, followed by isothermal sulfiding at 673 K for 90 min. (a) Co–O(573 K), (b) Co–O(1073 K), (c) Co–O(1273 K), (d) Co–O(1473 K). ●, Co_9S_8; ○, Co_3O_4; ▽, CoO; □, β-Co metal.

The γ peaks (a broad H_2S evolution peak associated with an H_2 consumption peak) are observed above 700 K, and peak maxima are seen at ca. 1160 K. The γ peak can be assigned to the reduction of Co_9S_8 to metallic Co. Quantitative TPR results are given in Table 5.

XRD patterns are shown in Fig. 12 for Co–O(T_c) sulfided up to 673 K at β = 6 K min^{-1}, followed by isothermal sulfidation for 90 min at 673 K. The cobalt oxides calcined at $T_c \geq 1073$ K clearly exhibit the presence of unsulfided crystalline CoO (2θ = 42.2°), while XRD peaks other than that due to Co_9S_8 are not detected for the sulfided Co–O(573 K). In addition, a weak peak due to β-Co metal (2θ = 44.2°) is observed for the sulfided Co–O(1473 K).

A subsequent H_2 treatment on the sulfided Co–O(T_c) for 60 min at 673 K resulted in a corresponding Co–S_{pro}(T_c) and caused reduction of unsulfided species as shown in Fig. 13. A peak due to metallic Co is obviously observed for Co–S_{pro}(1273 K) and Co–S_{pro}(1473 K).

DISCUSSION

Sulfided cobalt catalysts prepared from the same precursor cobalt oxides showed

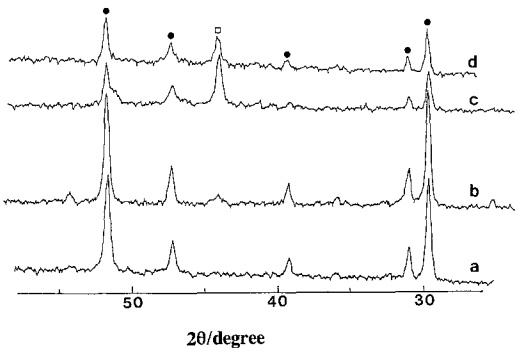

FIG. 13. X-Ray diffraction patterns of sulfided Co–O(T_c) (as shown in Fig. 12) subsequently H_2-treated for 60 min at 673 K, that is, Co–S_{pro}(T_c). (a) Co–O(573 K), (b) Co–O(1073 K), (c) Co–O(1273 K), (d) Co–O(1473 K). ●, Co_9S_8; □, β-Co metal.

different catalytic activities, depending on the sulfidation method: isothermal sulfidation or temperature-programmed sulfidation. It is instructive to consider the sulfidation mechanism of the precursor cobalt oxide by means of TPS.

Two kinds of catalytically active sites on sulfided cobalt catalysts for the hydrogenation of butadiene and the isomerization of 1-butene can be found. These were denoted "Co(L)" and "Co(H)", respectively (*4*). The catalytic activity of cobalt sulfide catalysts prepared from precursor cobalt oxides calcined at T_c by isothermal sulfidation, Co–S_{iso}(T_c), greatly increases at $T_c \geq$ 1473 K. The high activity is responsible for the formation of Co(H) sites. On the basis of the relationship between activities and selectivities in Tables 2 and 3, it is concluded that the active sites on Co–S_{pro}(> 973 K) are identical to Co(H) sites on Co–S_{iso} (1473–1573 K). The catalytic activities for both hydrogenation and isomerization in Figs. 2 and 3 indicate that the T_c dependence of the generation of Co(H) sites on Co–S_{pro}(T_c) is quite different from that on Co–S_{iso}(T_c).

Sulfidation Mechanism of Co_3O_4 to Co_9S_8

The TPS patterns (β = 10 K min^{-1}) of the cobalt oxides (Fig. 4) indicate two distinctly different kinds of sulfidation processes. One is typically observed in the TPS patterns for Co–O(573 K), in which sulfidation proceeds by consuming H_2S and H_2 concurrently. Similar TPS patterns are observed for the supported cobalt oxide such as CoO/SiO_2 (Fig. 5) at much lower temperatures. It has been reported for CoO/SiO_2 that cobalt species considerably segregate on the outer surface of SiO_2, forming ill-dispersed Co_3O_4 particles (*16*). The decrease in sulfidation temperature for CoO/SiO_2 is attributed predominantly to a smaller particle size of constituent Co_3O_4, compared with unsupported Co–O(573 K). The crystallite sizes of Co_3O_4 in CoO/SiO_2 and Co–O(573 K) were estimated to be about 7 and 14 nm from the linewidth of the XRD peak, respectively (*4*, *16*).

Another sulfidation process is seen in the TPS for Co–O(1573 K), in which sharp H_2 consumption and subsequent H_2 evolution are found around 700–900 K. Irrespective of the difference in the TPS pattern, the overall H_2S and H_2 consumptions in the temperature range 300 to 900 K correspond to the formation of Co_9S_8. The appearance of an H_2 evolution peak at ca. 800 K indicates the formation of Co metal as an intermediate on sulfidation of Co_3O_4 to Co_9S_8. Arnoldy *et al.* (*8*) also reported that large CoO and Co_3O_4 particles were sulfided via the intermediate formation of metallic Co in the inner parts of crystallites. The metallic Co might be surrounded by a dense Co_9S_8 skin where H_2 diffusion is much faster than H_2S diffusion. Indeed, the crystallite size of Co_3O_4 for Co–O(1573 K) is much larger than that for Co–O(573 K) (ca. 113 and 14 nm, respectively).

The TPS results at β = 2 K min^{-1} shown in Fig. 6 also provide more detailed information about the sulfidation processes of the precursor cobalt oxide to Co_9S_8 in the sulfidation temperature range 300 to 900 K. The simplified sulfidation scheme of Co_3O_4 to Co_9S_8 is represented in Fig. 14. The sulfidation mechanism responsible for the H_2S (S0–4) and H_2 (H0–4) peaks in Fig. 6 is interpreted as follows.

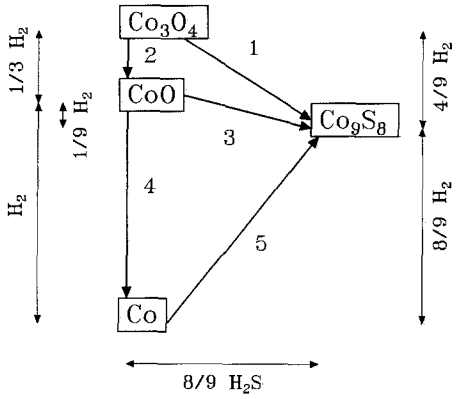

FIG. 14. Scheme for sulfidation of Co_3O_4 to Co_9S_8.

(1) $3Co_3O_4 + 8H_2S + 4H_2 \rightarrow Co_9S_8 + 12H_2O$
(2) $Co_3O_4 + H_2 \rightarrow 3CoO + H_2O$
(3) $9CoO + 8H_2S + H_2 \rightarrow Co_9S_8 + 9H_2O$
(4) $CoO + H_2 \rightarrow Co + H_2O$
(5) $9Co + 8H_2S \rightarrow Co_9S_8 + 8H_2$

The H_2S consumption peak, S0, is assigned to a direct sulfidation of Co_3O_4 to Co_9S_8 via reaction 1 in Fig. 14, since H_2S is a primary reactant via O–S anion-exchange reaction in the sulfidation temperature range 295–600 K (*8*). Such low-temperature sulfidation is considered to occur only on ultrafine cobalt oxide particles or topmost surface layers. Since H_2 consumption, H0, in this region is too small, the O–S exchange must be a dominant reaction. The following reaction sequences are, accordingly, conjectured here.

$$3Co_3O_4 + 8H_2S \rightarrow Co_9S_8 + 4(O) + 8H_2O \quad (1)$$

$$(O) + H_2 \rightarrow H_2O \quad (2)$$

or

$$4(O) + H_2S \rightarrow SO_3 + H_2O \quad (3)$$

$$SO_3 + O^{2-}_{\text{lattice}} \rightarrow SO_4^{2-} \quad (4)$$

The first step, reaction (1), denotes an anion-exchange process, where excess oxygen atoms (O) are evolved due to the reduction of Co^{3+} to Co^{2+}. Although most of the oxygen atoms are reduced by H_2 via reaction (2), some of the oxygen atoms are consumed in reactions (3) and (4), producing SO_4^{2-}. It has been shown that a significant amount of sulfate sulfur was detected by X-ray photoelectron spectroscopy for Co–O(573 K) sulfided below 473 K (*4*). The resulting sulfate anions are expected to be reduced by H_2 at higher temperatures in the TPS process.

Since the H_2 consumption in H1 exceeds the H_2S consumption in S1 for Co–O(573–773 K), the following sulfidation–reduction mechanism is proposed. Sulfidation of small cobalt oxide particles proceeds from the outer surface via O–S exchange (reaction 1 in Fig. 14) at first; subsequently H_2 reduction of the inner part of the oxide particles takes place, probably to CoO (reaction 2 in Fig. 14). The formation of similarly reduced core oxide has also been reported for the sulfidation of bulk MoO_3 (*18*). Once a cobalt sulfide skin is produced over the cobalt oxide particles, H_2 diffusion is anticipated to precede H_2S diffusion because of the passivating nature of the cobalt sulfide. On the other hand, a further increase in crystallite size of the cobalt oxide particles may prevent even diffusion of H_2 through the sulfide skin, since marked H_2 consumption in H1 does not appear for Co–O($\geq$ 973 K).

TPS patterns for Co–O(573–973 K) in Fig. 6 show that sulfidation of the cobalt oxide to Co_9S_8 is almost completed by the process of S2 and H2 [weak shoulders of S3 and H3 were observed for Co–O(973 K)]. Relatively small particles of cobalt oxide such as Co–O(573–973 K) are sulfided from the outer surface to the inner part. Subsequently, reduction to CoO by diffusion of H_2 through the sulfide skin competes with sulfidation of CoO to Co_9S_8 by diffusion of H_2S. Especially for Co–O(573 K), the reduced CoO core may react with H_2S, resulting in Co_9S_8 via reaction 3 (Fig. 14), since H_2S consumption in S2 is much larger than H_2 consumption in H2. On the other hand, for Co–O(973 K), it is necessary to consider the reduction of the inner part (H2), followed by growing a sulfide phase (S2). The larger crystallite size of the cobalt oxide results in a higher temperature shift of S2 as

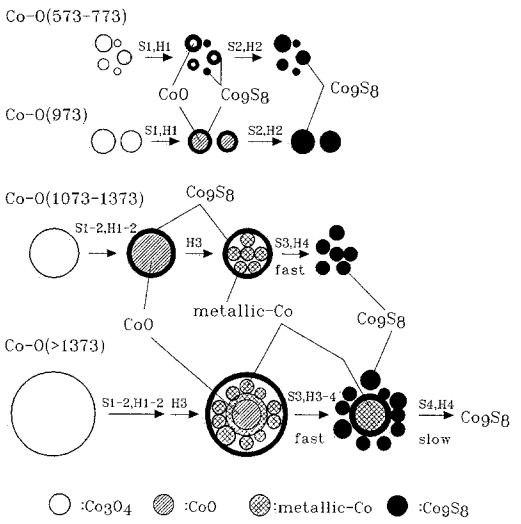

FIG. 15. Schematic diagrams of the mechanism of sulfidation of Co_3O_4 to Co_9S_8 for the precursor cobalt oxides calcined at various temperatures.

a consequence of increasing H_2S diffusion limitation. In accordance with this, S2 shifts to higher temperature from 624 K for Co–O(573 K) to 665 K for Co–O(973 K). A model for the sulfidation mechanism of Co_3O_4 to Co_9S_8 is schematically presented in Fig. 15.

If the above sulfidation mechanism is applicable to the cobalt oxide at $T_c > 973$ K, one might expect an additional temperature shift of S2. However, S2 cannot be observed for Co–O(> 973 K). Instead of S2, a set of strong H_2S consumption (S3) and H_2 consumption (H3) peaks appear at ca. 700 K for Co–O(1073–1573 K). As H3 always accompanies the H_2 evolution peak (H4), H3 is assigned to reduction of all of the CoO phase to metallic Co (reaction 4 in Fig. 14) and H4 is assigned to H_2 evolution by a subsequent reaction of H_2S with metallic Co (S3 and S4), producing Co_9S_8 and H_2 (reaction 5 in Fig. 14). Assuming that the H2 consumption in H3 is ascribed to the formation of metallic Co, both S3 and S4 can be attributed to the H_2S consumption in reaction 5. An important feature of S3 is that the appearance of S3 is synchronized with H3, whereas S4 shifts to 40–50 K higher temperature of H3.

Taking into account the above consideration, the following sulfidation mechanism is proposed for Co–O(1073–1573 K): In the case where the crystallite size of the cobalt oxide is larger than that for Co–O(573–973 K), H_2S (reaction 3) and H_2 (reaction 4) competitively react with the core oxide, which probably consists of CoO. The appearance of H4 instead of S2 indicates that reaction 4 (H_2) is superior to reaction 3 (H_2S) at the sulfidation temperature of ca. 700 K. Once metallic Co is formed, it is sulfided quickly to Co_9S_8 in S3 via reaction 5, especially for Co–O(1073 K) and Co–O(1173 K), until the sulfided layer becomes too thick to retard the diffusion of H_2S into the metallic core phase. One might expect that H_2S diffusion toward the core would be stimulated by producing a porous Co/CoO phase, which is formed by removal of the oxygen ions on reduction of CoO to metallic Co. It is reported that the reduction of Co_3O_4 to metallic Co results in a 30–50% decrease in Co particle size (*19*).

The shift of H4 to a higher temperature also suggests that an increase in the cobalt oxide particle size results in an increase in H_2S diffusion limitation. The complementary behavior of S3 and S4 implies that the sulfidation of metallic Co (reaction 5) occurs in two steps. The reduction–sulfidation reaction takes place in the first step (S3). If a reactive metallic Co core is large enough the re-formation of dense Co sulfide skin also inhibits H_2S diffusion. Thus, the S3-vs-T_c curve reveals a maximum at T_c between 1073 and 1173 K. In contrast, S4 appears at $T_c \geq 1073$ K and increases in intensity with increasing T_c. After all, the cobalt oxides are completely sulfided to Co_9S_8 in TPS up to 900 K. The most striking aspect of the present results is that the T_c dependence of S3 in Fig. 9 resembles the T_c dependence of the catalytic activities of Co–S_{pro}(T_c) in Figs. 2 and 3. Further details of the relationships between the sulfidation mechanism and the catalytic activities are discussed below.

Genesis of Highly Active Sites over Cobalt Sulfide Catalyst

Sulfidation of the precursor cobalt oxide to the sulfided cobalt catalyst [Co–$S_{pro}(T_c)$] can be simulated by the TPS procedures, as shown in Fig. 10. All of the cobalt oxides except Co–O(573 K) are sulfided mainly at an isothermal stage at 673 K. Considering the temperatures of the H_2S and H_2 consumption/evolution peaks (S0–4, H0–4) in the TPS experiment (β = 2 K min^{-1}) in Figs. 6–9, S0–2 and H0–2 (reaction 1 or reactions 2 and 3) are expected to occur during the temperature increase from 300 to 673 K. This is applicable to the TPS patterns of Co–O(573 K) and Co–O(973 K) in Fig. 10, while for the latter case the H_2S and H_2 consumptions are also observed at an early isothermal stage at 673 K. For Co–O(1073–1473 K), on the other hand, both H_2S and H_2 consumptions appear mainly at the same delay time after the beginning of the isothermal stage at 673 K. Especially for Co–O(1073 K) and Co–O(1273 K), the H_2 evolution peak appearing after the H_2 consumption peak should be assigned to H4 (reaction 5). Thus, the H_2S and H_2 consumption peaks at the isothermal stage are attributed mainly to S3 and H3, respectively (reactions 4 and 5). The quantitative TPS data are shown in Table 4. H_2S consumption decreases whereas H_2 consumption increases with increasing T_c for Co–O(1073–1473 K). This preponderance of the reduction suggests that all cobalt oxide particles are incompletely sulfided to Co_9S_8, and that the cobalt core phase (CoO or metallic Co) remains unsulfided.

Further confirmation of the presence of the unsulfided cobalt core phase after the sulfidation treatment in TPS is obtained from TPR and XRD experiments. The TPR results in Fig. 11 and Table 5 show that CoO phase, which is reduced at ca. 600 K, is estimated to comprise 1.3 and 4.3% of all Co atoms for Co–O(1273 K) and Co–O(1473 K), respectively. Assuming that all of the cobalt oxides (Co_3O_4) are transformed into Co_9S_8, CoO, and metallic Co by reacting with H_2S and H_2, the fractions of Co atoms for Co_9S_8, CoO, and metallic Co phases are roughly estimated to be 95:0–1:2–5, 91:1–2:6–8, and 87:4–5:9–18 for Co–O(1073 K), Co–O(1273 K), and Co–O(1473 K), respectively. The presence of the unsulfided cobalt core phase indicates that the transformation of the cobalt oxide to Co_9S_8 eventually terminates before reaction 4 and especially reaction 5.

The TPS results in Fig. 10 simulating Co–$S_{pro}(T_c)$ lead us to conclude that the precursor cobalt oxides for Co–O($\leq$ 973 K) are completely sulfided to Co_9S_8 via reaction 1 or reactions 2 and 3, whereas Co–O($\geq$ 1073 K) are sulfided mainly via intermediate formation of metallic Co (reactions 4 and 5). The difference in the diffusion limitations between H_2S and H_2 can be proposed to account for the differences in the sulfidation step of Co_3O_4 to Co_9S_8 as discussed previously. Such an abrupt change in the sulfidation properties as observed between Co–O($\leq$ 973 K) and Co–O($\geq$ 1073 K) may not be accounted for by only an increase in the crystallite size of the cobalt oxide [64 and 79 nm for Co–O(973 K) and Co–O(1173 K), respectively]. An additional explanation is a significant decrease in the BET surface area and an increase in the crystallite size of the cobalt oxide at $T_c \geq$ 1073 K as shown in Table 1. Surface area and crystallite size of the cobalt oxide may influence the sulfidation mechanism of the precursor cobalt oxide, that is, direct sulfidation to Co_9S_8 or via intermediate formation of metallic Co. The boundary condition that determines the sulfidation mechanism is probably the case between Co–O(973 K) and Co–O(1073 K).

The results of the activities for both hydrogenation and isomerization shown in Figs. 2 and 3 indicate that Co(H) sites can be generated most effectively for Co–S_{pro}(1173–1373 K). As proposed in the previous report (*4*), the cobalt metal overlayers modified by sulfur are responsible for the formation of Co(H) sites. This is in ac-

cord with the generation of "type B" catalyst from H_2 reduction of a mixture of CoS and CoO (*5*). In this case, Co(H) sites correlate with the formation of unsulfided cobalt oxide core phase within the passivating Co_9S_8 layer in the cobalt catalyst particle on sulfidation. By subsequent H_2 treatment at 673 K, the unsulfided cobalt core phase is reduced to metallic Co, followed by diffusion of surface sulfur anions into the metallic Co phase. This results in the production of a sulfur-deficient metallic surface layer, that is, Co(H) sites.

The amount of unsulfided cobalt core phase increases in the order Co–O(1073 K) < Co–O(1273 K) < Co–O(1473 K) as described previously. According to the interpretation of Co(H) site formation, one might expect that the higher catalytic activity would be obtained when the cobalt sulfide catalyst was prepared from the cobalt oxide calcined at the higher temperature. However, the cobalt sulfide catalysts ($Co–S_{pro}$) exhibit an activity maximum at T_c = 1373 K for hydrogenation and at T_c = 1173 K for isomerization. The obvious difference in the T_c dependence between the activities [i.e., the amount of Co(H) sites] and the amount of unsulfided cobalt phase is ascribed to the difference in the reactivity of the unsulfided cobalt phase. Such a large metallic Co phase for the sulfided Co–O($\geq$ 1473 K) is not completely transformed to the sulfur-deficient metallic surface layer [Co(H) sites], due to the limitation of the incorporation of the surface sulfur anions during H_2 treatment at 673 K. This effect results in the decrease in the catalytic activities for $Co–S_{pro}$($\geq$ 1473). This also explains the correlation between the T_c dependence of the catalytic activities and the intensity of S3 in Fig. 9. The intensity of S3 may correlate with the reactivity of the metallic Co phase.

The variation in the catalytic activities of $Co–S_{pro}(T_c)$ with those of $Co–S_{iso}(T_c)$ (Figs. 2 and 3) shows that $Co–S_{pro}(T_c)$ is considerably higher in activity than $Co–S_{iso}(T_c)$ and the extent of enhancement amounts to ca. 10-fold at T_c = 1173–1373 K for hydrogenation and isomerization. A shift of optimum T_c to lower temperature is also found for $Co–S_{pro}(T_c)$ compared with $Co–S_{iso}(T_c)$. This is reasonable since the passivating Co_9S_8 layer is effectively formed on the outer surface of the cobalt oxide particle in a low sulfidation temperature range (<650 K). The formation of passivating Co_9S_8 layers for $Co–S_{iso}(T_c)$ prefers a larger crystallite size or a smaller surface area of the starting cobalt oxide, such as Co–O($T_c \geq$ 1473 K). As the sulfidation treatment is started at 673 K in $Co–S_{iso}(T_c)$, reduction by H_2 is fast enough to prevent formation of the passivating Co_9S_8 layer. The passivating sulfide skin is reported to consist of 5–10 layers of MoS_2 (ca. 3–6 nm in thickness) in the sulfided unsupported and supported MoO_3 systems (*18, 20*).

In case of a supported cobalt oxide, even for CoO/SiO_2 containing ill-dispersed Co_3O_4 prepared from cobalt nitrate, the crystallite size of Co_3O_4 is considerably smaller than that of the precursor cobalt oxides [e.g., Co–O(573 K)]. Therefore, formation of Co(H) sites cannot be expected, since small cobalt oxide particles might be readily sulfided to Co_9S_8 via O–S anion exchange (reaction 1) or a CoO intermediate (reactions 2 and 3) under the usual sulfidation conditions.

CONCLUSIONS

Sulfidation properties of precursor cobalt oxides calcined at various temperatures are investigated by using TPS. TPS results indicate two distinctly different kinds of sulfidation process. These are differentiated in terms of the presence of a metallic Co as an intermediate. The probability of sulfiding via the metallic Co intermediate depends on the surface area and crystallite size of the cobalt oxide and on the sulfidation temperature. It is suggested that the metallic Co is produced when the cobalt oxide particle is surrounded by a passivating Co_9S_8 skin. The difference in the diffusion limitations between H_2S and H_2 is proposed to account

for the differences in the Co_3O_4 to Co_9S_8 sulfidation process.

The sulfidation method strongly affects the catalytic properties of the resultant cobalt sulfide catalysts, as well as the calcination temperature of the cobalt oxide. The cobalt oxides sulfided by temperature-programmed sulfidation show high activities for hydrogenation and isomerization compared with those of prepared by the previously reported isothermal sulfidation method (*4*). TPS, TPR, and XRD results indicate that the cobalt oxide partially sulfided at 673 K by temperature-programmed sulfidation (consists of unsulfided cobalt core phases such as CoO or metallic Co) shows high activities. The unsulfided cobalt core is subsequently reduced by H_2 treatment to the metallic Co phase. The high catalytic activities are interpreted in terms of the formation of a surface cobalt metal overlayer modified with sulfur.

ACKNOWLEDGMENTS

The author is greatly indebted to Professor Jacob A. Moulijn (Delft University of Technology) for many helpful suggestions in setting up the TPS/TPR apparatus. Thanks are due Dr. Y. Akai (Idemitsu Kosan Co., Ltd.) for helpful discussion.

REFERENCES

1. Vissers, J. P. R., de Beer, V. H. J., and Prins, R., *J. Chem. Soc. Faraday Trans. 1* **83,** 2145 (1987).
2. Ledoux, M. J., Michaux, O., Agostini, G., and Panissod, P., *J. Catal.* **96,** 189 (1985).
3. Duchet, J. C., van Oers, E.M., de Beer, V. H. J., and Prins, R., *J. Catal.* **80,** 386 (1983).
4. Okamoto, Y., Nagata, K., Imanaka, T., Inamura, K., and Takyu, T., *Appl. Catal.,* to appear.
5. George, M., Moyes, R. B., Ramanarao, D., and Wells, P. B., *J. Catal.* **52,** 486 (1978).
6. Scheffer, B., de Jonge, J. C. M., Arnoldy, P., and Moulijn, J. A., *Bull. Soc. Chim. Belg.* **93,** 751 (1984).
7. Arnoldy, P., van den Heijkant, J. A. M., de Bok, G. D., and Moulijn, J. A., *J. Catal.* **92,** 35 (1985).
8. Arnoldy, P., de Booys, J. L., Scheffer, B., and Moulijn, J. A., *J. Catal.* **96,** 122 (1985).
9. Scheffer, B., Dekker, N. J. J., Mangnus, P. J., and Moulijn, J. A., *J. Catal.***121,** 31 (1990).
10. Tsubomura, T., Kimura, K., Kaya, K., Tanaka, J., and Nagakura, S., *Bull. Chem. Soc. Japan* **37,** 417 (1964).
11. Arnoldy, P., and Moulijn, J. A., *J. Catal.* **93,** 38 (1985).
12. Lambert, J. M., Jr., Simkovich, G., and Walker, P. L., Jr., *Fuel* **59,** 687 (1980).
13. Kuznetsov, V. G., Sokolova, M. A., Palkina, K. K., and Popova, Z. V., *Inorg. Mater.* **1,** 617 (1965).
14. Rosenqvist, T., *J. Iron Steel Inst.* **176,** 37 (1954).
15. McKinley, J. B., *in* "Catalysis" (P. H. Emmett, Ed.), Vol. 5, p. 452. Reinhold, New York, 1957.
16. Okamoto, Y., Nagata, K., Adachi, T., Imanaka, T., Inamura, K., and Takyu, T., *J. Phys. Chem.* **95,** 310 (1991).
17. Wimmers, O. J., Arnoldy, P., and Moulijn, J. A., *J. Phys. Chem.* **90,** 1331 (1986).
18. Sanders, J. V., and Pratt, K. C., *J. Catal.* **67,** 331 (1981).
19. Castner, D. G., Watson, P. R., and Chan, I. Y., *J. Phys. Chem.* **94,** 819 (1990).
20. Pratt, K. C., Sanders, J. V., and Christov, V., *J. Catal.* **124,** 416 (1990).